PHYSICAL REVIEW B VOLUME 14, NUMBER 1 1 JULY 1976

Neutron scattering study of the diffuse critical scattering associated with the Verwey transition in magnetite (Fe_3O_4)†

S. M. Shapiro, M. Iizumi,* and G. Shirane
Brookhaven National Laboratory, Upton, New York 11973
(Received 9 February 1976)

The temperature-dependent diffuse critical scattering associated with the Verwey ordering ($T_V = 122$ K) in magnetite (Fe_3O_4) is extensively studied by means of neutron scattering experiments. The q dependence of the scattering reveals that it is planar in nature and shown to arise from one-dimensional (1-D) correlations along a cube edge. The diffuse scattering is observable at high temperatures ($T - T_V < 100$ K) and increases rapidly as T_V is approached. Near T_V, the spotlike 3-D critical scattering studied by Fujii *et al.* appears. At T_V the diffuse scattering shows an abrupt decrease and is absent below. Inelastic studies show that the diffuse scattering is predominantly inelastic and couples strongly to the transverse acoustic phonons propagating with q in the plane of diffuse scattering. The spectra are interpreted via a pseudospin–phonon theory and the significant parameters are derived.

I. INTRODUCTION

Magnetite is the oldest known magnetic material and one of the most thoroughly studied.[1] In addition to the ferrimagnetic ordering of the iron sublattices at $T = 850$ K, Fe_3O_4 undergoes a first-order phase transition near $T_V = 123$ K, where there is a charge ordering of the Fe^{2+} and Fe^{3+} ions within the octahedral sites of the cubic inverse spinel structure.[2] Verwey originally proposed as an ordering scheme an alternation of Fe^{2+} and Fe^{3+} layers along [001], which is the direction of the magnetization.[2]

Recent experimental evidence[3-6] has caused a rethinking of the Verwey ordering. Samuelsen *et al.*,[3] by neutron diffraction, and Yamada *et al.*,[4] by electron diffraction, disclosed the existence of the superlattice reflections below T_V, and Samuelsen *et al.* noted that the satellite intensities were proportional to the square of the reciprocal-lattice vectors, which suggests that the observed intensity is mainly due to atomic displacements and is not of magnetic origin. More recently Fujii *et al.*[7] studied the spotlike critical scattering above T_V which appears at $(h, 0, l \pm \frac{1}{2})$ $(h, l = 4n)$ positions in reciprocal space which become Bragg peaks below T_V. They applied Yamada's model[8] to explain the critical scattering and found good agreement with their observations. This model predicts an ordering of the Fe^{2+} and Fe^{3+} ions *within* the (001) atomic planes. Additional evidence in general support of this ordering scheme was supplied by Shirane *et al.*,[9] who studied the low-temperature structure of magnetite and found the (002) Bragg reflection was missing, proving therefore that the Verwey ordering cannot be correct. However, the Yamada model fails to explain the observed magnetic intensities[9] and does not allow for mixed integer reflections.[10] Consequently, a more detailed refinement of the model is necessary.

In addition to the spotlike scattering studied by Fujii, there exists a type of critical scattering observable over a broader region in q space and over a larger temperature range. Chiba *et al.*,[11] by means of electron diffraction, first observed this diffuse scattering above T_V. Their observations are in substantial agreement with our results, shown in Fig. 1, except for the region near (0, 4, 4). In Fig. 1, the circles represent the Bragg points of the high-temperature phase and the oval curves schematically represent the regions where the diffuse scattering is observed. Fujii *et al.*[7] also observed this diffuse scattering in their neutron experiment, but it was not extensively studied, nor was its relationship to the spotlike critical scattering understood. It is the purpose of the present investigation to study in detail the $\vec{q}$, energy, and temperature dependence of the diffuse scattering and attempt to explain its role in the Fe^{2+} and Fe^{3+} ordering in magnetite.

II. EXPERIMENTAL

The experimental results presented below were performed on the synthetic single crystal used in the previous neutron experiment[7] and kindly provided by S. Chikazumi, M. Matsui, and S. Todo. The high-temperature crystal symmetry is the cubic inverse spinel ($O_h^7 \equiv Fd3m$) with a lattice constant $a = 8.386$ Å at 130 K. The cylindrical sample was 10 mm in diameter and 15 mm in height, with the cylindrical axis parallel to the [111] direction. The mosaic of this crystal was 12 min at 130 K. All measurements were made in the [010] or the [01$\bar{1}$]

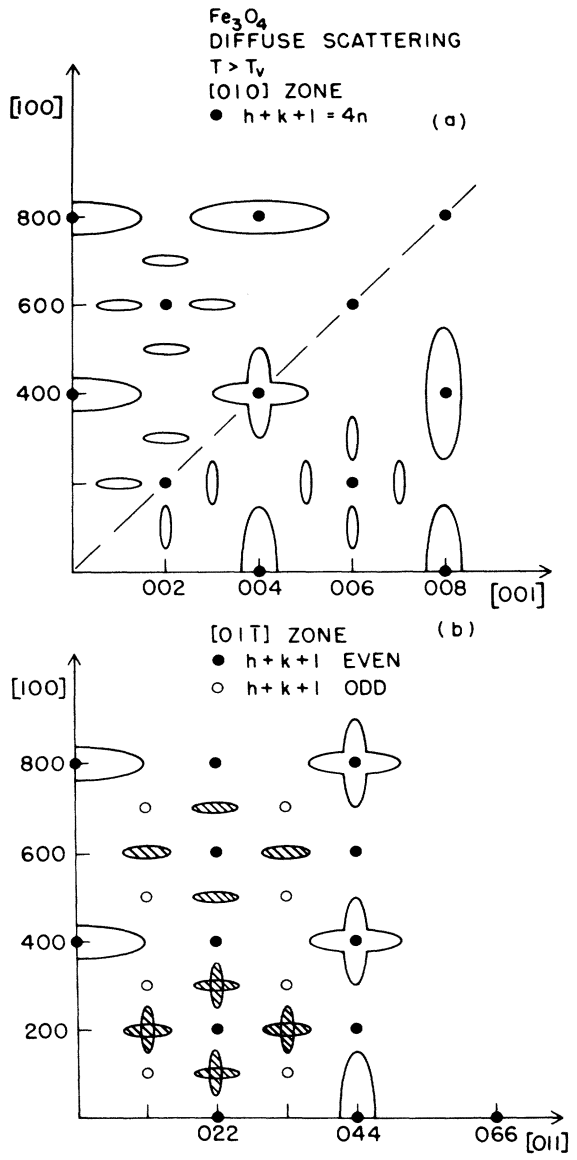

FIG. 1. Schematic representation of the location of the diffuse scattering in (a) the [010] zone. The dots are the allowed Bragg peaks and the dashed line at 45° breaks up the quadrant into two regions which are equivalent owing to cubic symmetry. (b) The [01$\bar{1}$] zone. The solid and open circles are allowed Bragg peaks with h, k, l all even or all odd, respectively. The hatched regions are near-zone boundaries.

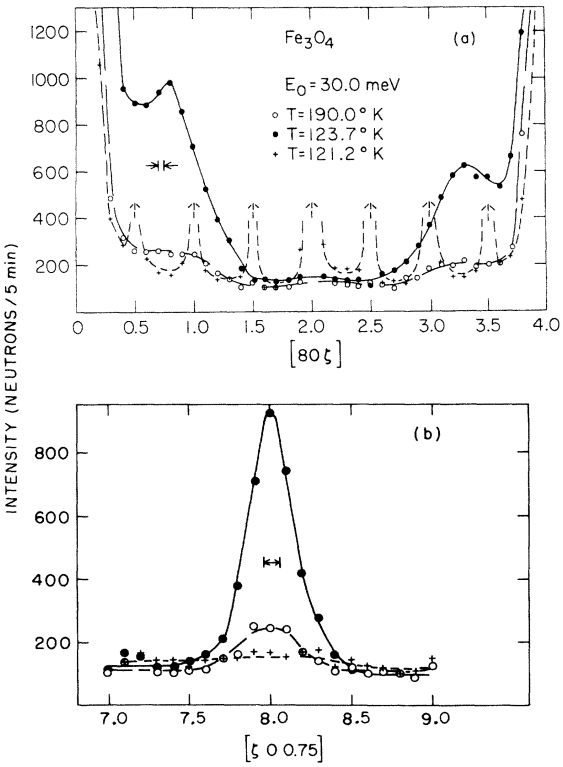

FIG. 2. Diffuse scattering observed in the [010] zone. The small vertical lines indicate the size of the instrumental resolution. (a) Scan along [80ζ]. (b) Scan perpendicular to (a), along [ζ,0,0.75].

zones. After the experiment of Fujii *et al.*[7] and just prior to the present experiment, the crystal was used in a study of the ferromagnetic ordering and kept at 850 K in vacuum for approximately 10 weeks,[12] resulting in a slight change of the Verwey transition temperature. T_V as measured in our experiment is 122.3 K on cooling and 122.5 K on heating, which is to be compared with 122.6 and 122.8 K on cooling and heating as measured by Fujii *et al.*[7] prior to the heat treatment.

Another important change is the intensity of the critical scattering studied by Fujii *et al.*[7] After the heat treatment, the spotlike critical scattering is weaker, for the same $T - T_V$, than that reported in Ref. 7. Additionally, the broad diffuse scattering observed in Ref. 7 does not show such pronounced peaks as seen in the present experiment (see Fig. 2). Although the cause of these changes is not presently understood, it is likely that a change in the oxygen content as a result of the annealing at high temperatures could cause changes in T_V and related critical behavior.

The sample was placed in an aluminum can filled with He gas and mounted in a Cryogenics Associates CT-14 flow cryostat. The temperature was controlled and regulated to within ±0.01 K.

The neutron scattering experiments were performed at the Brookhaven High Flux Beam Reactor. Incident neutron energies of 13.7, 14.8, 30, or 41 meV were employed, depending upon the demands of the energy and Q range. Several energy scans were also performed with a fixed analyzer energy of 14.8 meV and a variable incident energy. In

all cases a pyrolytic graphite monochromator and analyzer were used and a pyrolytic graphite filter was used to eliminate higher-order contamination. Horizontal collimation of 20 or 40 min was used, depending upon the resolution and intensity needs.

III. EXPERIMENTAL RESULTS

A. $E=0$ scattering

Figure 2(a) shows the results of our $E=0, q$ scans along the $[80\zeta]$ direction at several temperatures. At the temperature just above $T_V = 122.5$ K, the intensity is broadly distributed along $[00\zeta]$. The spotlike scattering studied by Fujii *et al.*[7] is weak at this temperature and would appear as bumps on this broad curve at $\zeta = \frac{1}{2}$, 1, $\frac{3}{2}$, 2, $\frac{5}{2}$, 3, and $\frac{7}{2}$. On heating, there is an overall decrease in intensity with little change in shape. The peaks observed in this scan appear at incommensurate positions along ζ and are not obviously related to the appearance of the new Bragg peaks in the low-temperature phase. Figure 2(b) shows a scan along the $[\zeta\, 0\, 0.75]$ direction, perpendicular to the ridge of scattering in Fig. 2(a). The scattering centers sharply about $\zeta = 8.0$, indicating the intensity in the [010] zone is confined to the ridge extending along the $[00\zeta]$ direction. This ridge has a q width larger than our instrumental resolution. It is important to determine the q extent of this scattering perpendicular to the [010] scattering plane. By tilting the crystal about $[00l]$, the scattering plane can be changed to contain a component in the $[0k0]$ direction, so that the distribution of the scattering perpendicular to the [100] direction can be studied. We observed that the intensity extends nearly uniformly in the plane perpendicular to the cube axis [100]. These observations indicate that the diffuse scattering originates from the one-dimensional (1-D) correlations along ⟨100⟩ in the real space. The correlation perpendicular to these directions extends over a much larger distance, as given by the relative q widths in Figs. 2(a) and 2(b). At temperatures less than T_V, the diffuse scattering has disappeared and new Bragg peaks appear at $\zeta = \frac{1}{2}$, 1, $\frac{3}{2}$, 2, $\frac{5}{2}$, 3, and $\frac{7}{2}$, consistent with a doubling of the cell along the [001] direction.

Figure 3 shows $E=0$ scans in the $[01\bar{1}]$ zone. The diffuse scattering exhibits behavior similar to that in the [010] zone. It extends out along $[h\zeta\zeta]$ and is narrow along the $[\zeta 00]$ direction. The scattering was observed for $h = 1, \ldots, 8$, in agreement with the electron diffraction results,[11] except near (0, 4, 4), where the electron diffraction results show an X-shape scattering and we see a continuous streak along the ⟨100⟩ direction. By tilting the crystal we also observed the diffuse scattering along the two other cube directions intersecting the $[01\bar{1}]$ zone at 45°.

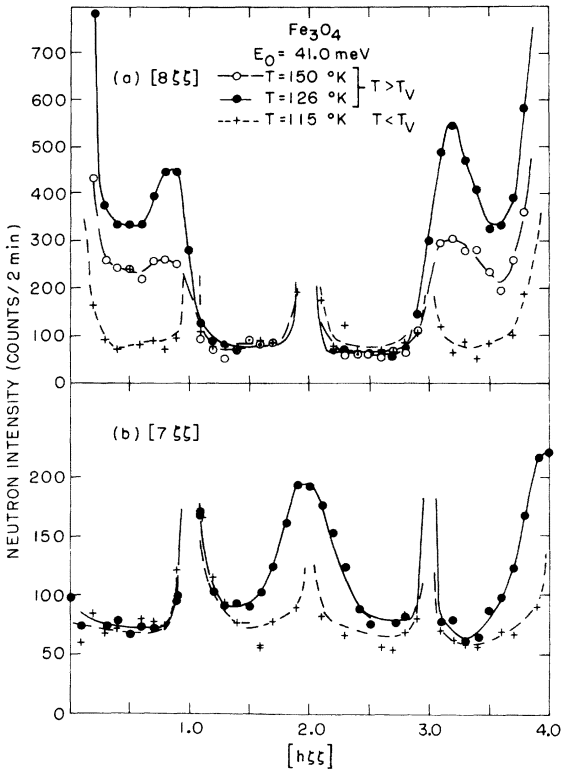

FIG. 3. Diffuse scattering observed in the $[01\bar{1}]$ zone. (a) Scan along $[8\zeta\zeta]$. (b) Scan along $[7\zeta\zeta]$ at $T = 126$ and 115 °K.

Figures 1(a) and 1(b) illustrate schematically the location of the diffuse scattering observed in the [010] and $[01\bar{1}]$ zones, respectively. The strongest scattering is observed along the $[h0\zeta]$ and $[h\zeta\zeta]$ directions for even values of h, but scattering is also observed for mixed, even-odd integers corresponding to zone boundaries. The general tendency of the intensity follows Q^2 dependence ($\vec{Q}$ is the reciprocal-space vector) and implies that the origin of the diffuse scattering is the atomic displacement. It is readily seen that the atomic displacements giving rise to the scattering are transverselike.

The observed diffuse scattering is indeed critical, since it tends to diverge as T_V is approached. Figure 4 shows the temperature dependence of the (8, 0, 0.75) point in reciprocal space. There is considerable intensity at $T = 160$ K and it increases as T_V is approached and falls sharply as the Verwey transition occurs.

B. Inelastic scattering

Energy analysis of the scattering taken at Q values where the diffuse scattering is strong reveals

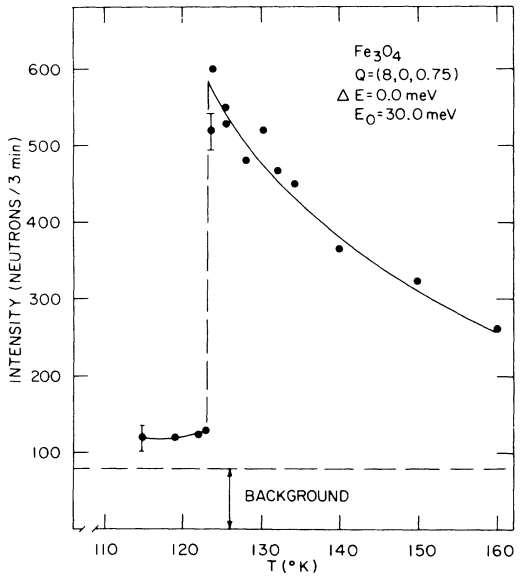

FIG. 4. Temperature dependence of the diffuse scattering measured at $\vec{Q} = (8,0,0.75)$.

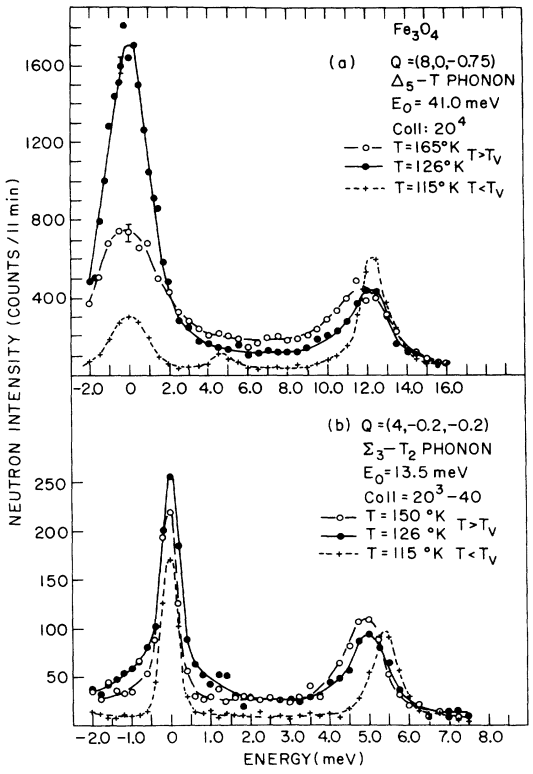

FIG. 5. Inelastic spectra measured at several temperature. (a) Δ_5 transverse phonon. (b) Σ_3-T_2 phonon.

interesting line shapes. Figure 5(a) shows several spectra at (8, 0, − 0.75) for several temperatures taken with 41.0-meV incident neutron energy. Peaks at about 12 meV are the scattering creating the transverse acoustic Δ_5 phonons.[7,13] The atomic displacements associated with this phonon are pointed out to be relevant to the lattice stability at T_V by Yamada,[8] based on the measurements by Fujii *et al.*[7] The lowest temperature shown in the figure, $T = 115$ K, is less than T_V, and the diffuse scattering has disappeared. At this temperature the intensity about $E = 0$ is a measure of the incoherent scattering and the phonon line shape is determined by the Gaussian resolution function of the spectrometer.[14] The intensity between $E = 0$ and the phonon is the background level of the experiment. [The additional peak near $E = 5.0$ meV is an acoustic phonon with $\vec{q}$ measured from the (8, 0, 0.5) reciprocal-lattice point of the low-temperature phase.] For temperatures greater than T_V, there is an increase in the central peak intensity, as discussed above, and an asymmetry of the phonon line shape develops. In addition, a significant amount of intensity appears between the phonon and the central peak. As T is further increased, the distortion of the phonon line shape becomes more severe, the intensity in the intermediate energy range increases, and the central peak decreases. Because of the poor instrumental resolution for this incident neutron energy, no energy width of the central peak is observed.

Figure 5(b) shows similar spectra taken at (4, − 0.2, − 0.2) with considerably higher instrumental resolution. In this case, the transverse-acoustic Σ_3 phonon propagating along the [011] direction with the principal component of the polarization in the direction of [100] is involved. The low-temperature data ($T = 115$ K) show a resolution-limited central peak owing to the incoherent scattering of the sample and a phonon peak at $E = 5.5$ meV whose linewidth is accounted for by the instrumental resolution. Between 0 and 5.0 meV, the intensity level is that of background. For $T > T_V$, the phonon line shape is distorted and intensity has built up at intermediate energies, as observed above. After subtracting the incoherent scattering we observe a line width of the central peak of $\Delta E = 1.5$ meV at $T = 126$ K which is considerably broader than the instrumental resolution of 0.5 meV. As T is increased further, the central peak broadens and its intensity decreases. We can now state that the diffuse scattering observed in the $E = 0, q$ scans discussed earlier is totally inelastic (aside from the incoherent scattering) and its linewidth broadens as $T - T_V$ increases. From the appearance of the spectra, we conclude that an interaction exists between the fluctuations which give rise to the central peak and the phonons. The high-resolution study was restricted to small q around (4, 0, 0) because of

the lower incident energy required. The more predominant observation of the interaction was possible only by using higher incident energy with poorer resolution. The fixed E_F scan is a favorable compromise between the two. A result of such a scan will be used in a later section in order to compare with a model.

Transverse-acoustic phonons propagating along [001] and [011] directions, both of which are contained in the plane of diffuse scattering and have their principal component of the polarization vector along [100], exhibit asymmetric line shapes. Transverse-acoustic phonons propagating in directions where no diffuse scattering is observed have normal resolution-determined line shapes and no observable linewidth. In particular, the transverse-acoustic Σ_4 phonon with the principal polarization component along the $[01\bar{1}]$ direction shows no interaction. We could not observe any anomaly in optic phonons. We may extrapolate our observation by saying that all the phonons with wave vectors lying the the ΓKWX plane ($q_x = 0$) and transforming according to the Γ_2 irreducible representation of the point group of C_s (or m) interact with the central component.

IV. DISCUSSION

A. $E=0$ scattering

The observed diffuse scattering has been shown to occur in planes of reciprocal space, which implies one-dimensional correlations in real space. A study of crystal structure does not reveal any obvious 1-D-like atomic correlations, but 1-D-like correlations have been observed in $BaTiO_3$ and $KNbO_3$, where there also is no *a priori* reason to expect them.[15] We interpret our results by calculating the dynamical structure factor with an assumed model for the displacements and comparing it with experiment. The intensity of the scattered neutrons is proportional to the square of the dynamical structure factor,

$$I(\vec{Q}_{hkl}) \propto |F(\vec{Q}_{hkl})|^2 = \left| \sum_i b_i (\vec{Q}_{hkl} \cdot \vec{\Delta}_i)\, e^{i \vec{Q}_{hkl} \cdot \vec{r}_i} \right|^2 ,$$

where the $\vec{\Delta}_i$'s are the atomic displacements which are taken from the model Yamada[8] used to explain the spotlike critical scattering. b_i is the nuclear scattering length of atom i and r_i is its position within the cell. The scattering vector is $\vec{Q}_{hkl} = G_{hkl} + \vec{q}$, where G_{hkl} is the reciprocal-lattice vector of the Brillouin-zone center defined by h, k, and l, and $\vec{q}$ is the wave vector of the displacements. If we assume that the correlations along [001] consist of four octahedral layers and the associated oxygen and tetrahedral iron atoms and by appropriately choosing the initial phase,[16] we obtain the curve for the calculated diffuse scattering given in Fig. 6, where it is compared with the observed data along the $[80\zeta]$ direction. An important difference is that the calculation shows the intensity at (8, 0, 0) and (8, 0, 4) is a minimum, whereas the experiment suggests a maximum. The agreement, however, is reasonable for this direction, considering the uncertainties in the model. We now see that the peaks in the diffuse scattering do not directly reflect the structure of the low-temperature phase as does the spotlike scattering, but their positions in reciprocal space are fundamentally related to the displacements contained in the Yamada model.[8] The agreement along other $[h0\zeta]$ and $[h\zeta\zeta]$ directions is only as good as the Yamada model in predicting the intensities of the critical spotlike scattering. The Yamada model is in poor agreement with the observed scattering for $[h0\zeta]$ when h is odd.

We can make additional qualitative statements based upon the knowledge of the low-temperature Bragg intensity observations.[9,10] The intensity of the diffuse scattering in a given Brillouin zone correlates with the satellite peaks observed in that zone below T_V. The regions where strong intensities are observed above T_V become strong Bragg peaks below T_V. This suggests that when a more detailed model of the atomic distortions required for the low-temperature symmetry is available, the q dependence of the diffuse scattering will also be explained.

In Fig. 7 we plot the reciprocal of the observed $E = 0$-meV intensity (multiplied by the temperature to account for the occupation factor) vs temperature. The diffuse scattering observed at (8, 0, 0.75) is the solid line, and the dashed line corresponds to the spotlike critical scattering studied by Fujii

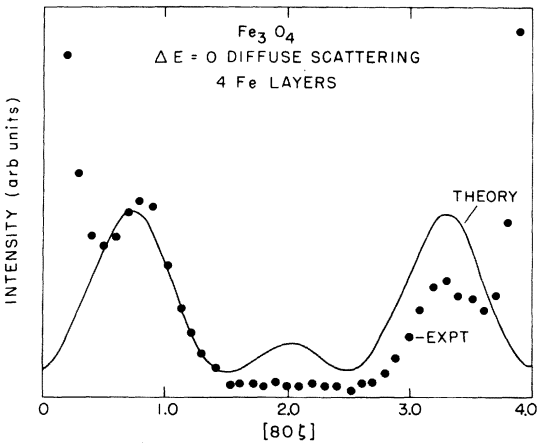

FIG. 6. Measured diffuse scattering along $[80\zeta]$ compared with the theoretical curves.

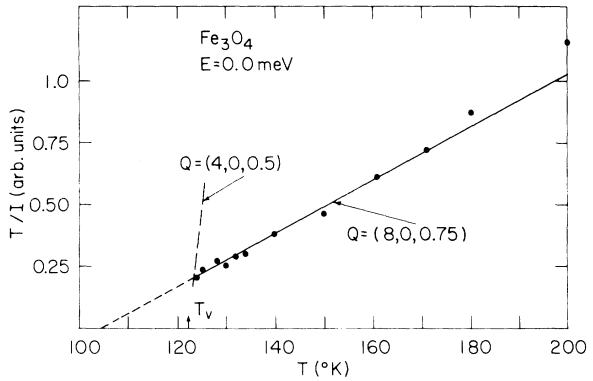

FIG. 7. Temperature dependence of the inverse intensity of the diffuse scattering (solid line) compared with the spotlike scattering measured in Ref. 7.

et al.[7] The spotlike scattering is observable only over a small temperature range $T - T_V < 4°$, whereas the diffuse critical scattering studied here is observable for $T - T_V < 80$ K. This behavior is reminiscent of observations in 1-D magnetic systems.[17] There, the planar diffuse scattering originates from 1-D correlations along the magnetic chains and is present at temperatures far from T_V. As the system cools the correlation length along the chains becomes so large that even a small 3-D interchain interaction can cause an ordering among the chains and additional critical scattering occurs. Eventually, the interchain interactions drive the transition. Such is the case in Fe_3O_4, although the chains are not as apparent as in the magnetic case. The broad diffuse scattering corresponds to the 1-D *intra*chain interactions and the spotlike scattering results from the *inter*chain interaction.

B. Inelastic scattering

We have seen that the energy spectrum of the diffuse scattering consists of a broad central peak and phonon peaks with an interaction between them. This spectral line shape suggests that there are two types of interacting dynamical variables, phonon and pseudospin, which take part in the scattering. Recently, the dynamical properties of the pseudospin-phonon coupled system have been extensively studied[18,19] and they have successfully been applied to the structural phase transitions in potassium dihydrogen phosphate (KDP),[20] in ND_4Br,[21] and cooperative Jahn-Teller phase transitions.[22]

Yamada[8] pointed out the importance of the interaction between the charge density fluctuations at the octahedral sites of magnetite and the phonons. He showed that the charge density mode at an octahedral unit cell involving four B-site irons is described by Ising spins, and there is a bilinear coupling between phonons and pseudospins. The microscopic Hamiltonian used to describe the coupled system is[18]

$$\mathcal{H} = \frac{1}{2}\sum_{\vec{q},s}\left[P_{\vec{q},s}+\omega_0^2(\vec{q},s)\,Q_{\vec{q},s}^2\right] - \frac{1}{2}\sum_{ij}J_{ij}\sigma_i\sigma_j + \sum_{\vec{q},s,j}\frac{\omega_0(\vec{q},s)}{\sqrt{N}}\,g_{\vec{q},s}\,Q_{\vec{q},s}\,\sigma_j\,e^{i(\vec{q}\cdot\vec{r}_j)}. \quad (1)$$

$Q_{\vec{q},s}$ is the normal coordinate of the phonon mode with wave vector $\vec{q}$, and $P_{\vec{q},s}$ is its conjugate momentum; s is the branch index. $\omega_0(\vec{q},s)$ is the characteristic frequency of this mode. σ_i represents the pseudospin variable used to describe the spin configuration of the octahedral iron site i. J_{ij} is the pair interaction between two spins and $g_{\vec{q},s}$ is the coupling between the spin and the phonon.

The scattered intensity for this system is given by

$$\frac{d^2\sigma}{d\Omega\,d\omega} \propto N\sum_s F_N^s(\vec{Q})\,\phi_{QQ}(\vec{q},\omega)\ . \quad (2)$$

In Eq. (2), $F_N^s(\vec{Q})$ is the dynamical structure factor of the sth phonon and $\phi_{QQ}(\vec{q},\omega)$ is the spectral function

$$\phi_{QQ}(\vec{q},\omega) = \int\langle Q_{\vec{q},s}(0)\,Q_{-\vec{q},s}(t)\rangle\,e^{i\omega t}\,dt\ . \quad (3)$$

There are several important assumptions involved in using the above expression. Firstly, we assume that the critical scattering is only nuclear in origin and contains no magnetic contribution. This allows the neutron intensity to be described solely by ϕ_{QQ}. The second assumption is that we consider coupling only to the transverse-acoustic modes propagating in the plane of scattering, and not to any of the optic modes.

ϕ_{QQ} is given by Yamada *et al.*,[18]

$$\phi_{QQ}(\vec{q},\omega) = 2\omega_0^2(\vec{q})\,\gamma k_B T\left(\frac{g_{\vec{q}}}{\gamma J'_{\vec{q}}}\right)^2 \times\left\{\left[\omega^2-\omega_0^2(\vec{q})\left(1-\frac{g_{\vec{q}}^2}{J'_{\vec{q}}}\right)\right]^2 + \omega^2\left(\frac{\omega^2-\omega_0^2(\vec{q})}{\gamma J'_{\vec{q}}}\right)^2\right\}^{-1}, \quad (4)$$

with $J'_{\vec{q}} = k_B T - J_{\vec{q}}$; γ describes the relaxation process for an individual spin. We can apply Eq. (4) to the measured spectra and deduce values of the parameters. The least-squares procedure involving the instrumental normalization factor could not

successfully deduce five parameters (γ, $J_{\vec{q}}$, $g_{\vec{q}}$, ω_0, and scale factor) independently. We therefore employed the constraint

$$J_{\vec{q}}+g_{\vec{q}}^2=k_B T_c \tag{5}$$

and set T_c to 105 K from the intercept in Fig. 7. Parameters for two sets of data at $\vec{q}=(0, 0, 0.75)$ and $\vec{q}=(0, 0.2, 0.2)$ were least-squared fitted by Eq. (4), and the values of parameters obtained are given in Table I. Figure 8 shows the results of the fit for the Σ_3-T_2 phonon. The incoherent scattering and background were estimated from the 115 K data and are already subtracted from the data. The instrumental energy resolution is small compared with the intrinsic widths of both the central peaks and the phonon peaks, so that the detailed correction for the resolution function is not necessary. Although some systematic discrepancies remain between data and best-fit curves, the overall agreement is reasonably good. The parameters obtained at different temperatures agree with each other. This means that the temperature dependence of the spectra is well described by the spectral function (4) with almost temperature-independent parameters and a critical temperature of about 105 K. Parameters obtained at different $\vec{q}$ on different symmetry axes have somewhat different values; the spin relaxation (γ) is faster along the [011] direction than along [001] and the coupling between spins and phonons is stronger at large q along [001] than at small q along [011]. The reduced parameters, $\tilde{\omega}=\omega_0/\gamma k_B T$, $\tilde{\tau}=J_{\vec{q}}/k_B T_c$, are also given in the table in order to compare them with the classification in the paper of Yamada *et al.*[18] Both spectra observed fall in the intermediate relaxation case ($\tilde{\omega}\sim 1$) with weak spin-phonon coupling ($\tilde{\tau}\sim 1$). Yamada[8] used the energy widths of the spotlike critical scattering[7]

TABLE I. Values of parameters in the pseudospin-phonon system.

	$q=(0, 0, 0.75)$		$q=(0, 0.2, 0.2)$	
Q	$(4, 0, 3.25)$		$(4, -0.2, -0.2)$	
T (K)	126	150	126	150
γ	0.42	0.41	0.76	0.72
J_q (meV)	6.22	5.35	7.82	7.30
g_q [(meV)$^{1/2}$]	1.68	1.92	1.11	1.32
$\omega_0^2(\vec{q})$ (meV)	12.4	12.3	5.33	5.35
$\tilde{\omega}=\omega_0/\gamma k_B T$	2.7	2.5	0.65	0.57
$\tilde{\tau}=J_q/k_B T_c$	0.69	0.59	0.86	0.81
τ_σ (10^{-12} sec)	0.90	0.78	0.50	0.44

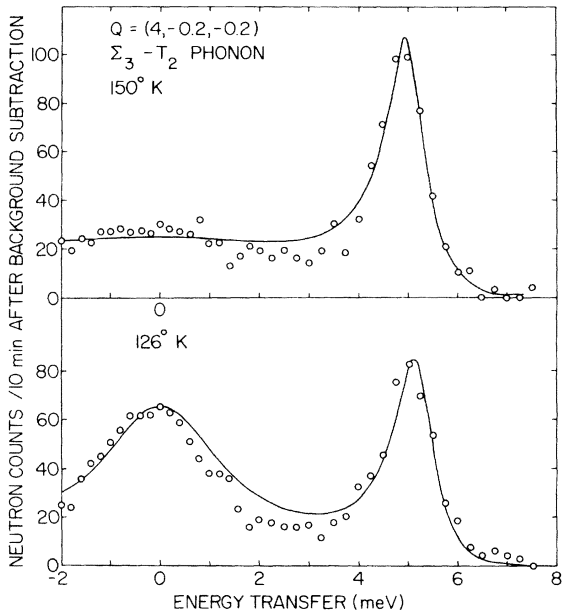

FIG. 8. Inelastic spectra of Σ_3-(transverse phonons) compared with a theoretical fit (solid line) described in the text. The background has been subtracted.

to estimate the minimum value of the relaxation time of the charge density fluctuation as 10^{-10} sec. But now that it has been revealed that the relevant scattering to the charge fluctuation at the octahedral sites is not that scattering but the diffuse scattering considered here, his estimate should be replaced by the values given in the last row of Table I. The charge density modes flip and relax with time constant of about 0.5×10^{-12} sec. This value disagrees with the relaxation time $\tau=1.1\times10^{-9}$ sec obtained by Mössbauer spectroscopy.[23] However, the electrical conductivity is fairly well understood by our fast relaxation time using the simple Einstein relation of electron hopping.

When Yamada[8] set forth his model, he took the phonons propagating along the [001] direction (Δ) as relevant to the Verwey transition. Experimental results presented thus far urge us to take a wider scope. We see that the acoustic phonons propagating with $\vec{q}$ in the $\vec{q}_x=0$ plane and having the principal component of polarization vectors along [100] couple with pseudospins. In particular, Σ_3 acoustic phonons are relevant but Σ_4 phonons are not. A common feature of the phonons which couple with the pseudospin modes is that they bring about a local rhombohedral distortion of the octahedral unit cells. This distortion seems to play an important role in the coupling of electron to phonons. The softening of the sound velocity of the c_{44} mode[24] may be taken to be the $\vec{q}\to 0$ limit of

the coupled system. In this limit ω_0 tends to 0 and the coupled system shifts to the fast-relaxation case ($\tilde{\omega} \sim 0.1$), where the coupled mode shows softening.

The neutron scattering cross section at $E=0$ is given by

$$\left(\frac{d^2\sigma}{d\Omega\, d\omega}\right)_{E=0} \propto |F_N(\vec{Q})|^2 \frac{2k_B T g_{\vec{q}}^2}{(k_B T - k_B T_c)^2 \gamma \omega_0^2(\vec{q})} , \tag{6}$$

and the width of the central peak is given approximately by

$$\gamma k_B (T - T_c) . \tag{7}$$

The integrated intensity I of the central peak is given roughly by the products of (6) and (7) and follows the temperature dependence:

$$1/I \propto (T - T_c)^{-1} . \tag{8}$$

This explains the behavior observed in Fig. 7. The intensity observed there is the integrated intensity rather than the peak intensity, because of the poor resolution.

From the point of view of this subsection the distribution in q space of $E=0$ scattering analyzed in Sec. IV B is described by

$$I(\vec{q}, E=0) \propto |F_N(\vec{Q})|^2 g_{\vec{q}}^2/\omega_0^2(\vec{q}) . \tag{9}$$

The one-dimensional nature of the correlation discussed above can be described in the dynamical language by asserting that the pseudospin-phonon coupling constant $g_{\vec{q}}$ is large only on the plane $q_x = 0$.

V. CONCLUSIONS

Strong inelastic diffuse scattering is observed in Fe_3O_4 and shown to be a result of 1-D correlations along a cube edge. This intensity increases as T_V is approached and eventually the 3-D interchain interaction becomes dominant and triggers the ordering. The latter interaction is evidenced by the spotlike critical scattering. There is a strong interaction between the observed central peak and the phonons propagating in the plane of diffuse scattering which is explained by a pseudospin-phonon coupling mechanism.

ACKNOWLEDGMENTS

The authors gratefully acknowledge helpful communications with S. Chikazumi, Y. Fujii, D. L. Huber, and Y. Yamada.

---

†Work performed under the auspices of the U.S. Energy Research and Development Administration.

*On leave from Japan Atomic Energy Research Institute, Tokai, Japan.

[1]S. Chikazumi, *Physics of Magnetism* (Wiley, New York, 1964).

[2]E. J. Verwey and P. W. Haayman, Physica (Utr.) 8, 979 (1941); E. J. Verwey, P. W. Haayman, and F. C. Romeijn, J. Chem. Phys. 15, 181 (1947).

[3]E. J. Samuelsen, E. J. Bleeker, L. Dobrzynski, and T. Riste, J. Appl. Phys. 39, 1114 (1968).

[4]T. Yamada, K. Suzuki, and S. Chikazumi, Appl. Phys. Lett. 13, 172 (1968).

[5]M. Rubinstein and D. W. Forester, Solid State Commun. 9, 1675 (1971); R. S. Hargrove and W. Kündig, Solid State Commun. 8, 303 (1970).

[6]S. Chikazumi, K. Chiba, K. Suzuki, and T. Yamada, in *Proceedings of the International Conference on Ferrites* (University of Tokyo Press, Tokyo, 1971), p. 595.

[7]Y. Fujii, G. Shirane, and Y. Yamada, Phys. Rev. B 11, 2036 (1975).

[8]Y. Yamada, AIP Conf. Proc. 24, 79 (1974).

[9]G. Shirane, S. Chikazumi, J. Akimitsu, K. Chiba, M. Matsui, and Y. Fujii, J. Phys. Soc. Jpn. 39, 949 (1975).

[10]M. Iizumi and G. Shirane, Solid State Commun. 17, 433 (1975).

[11]K. Chiba, K. Suzuki, and S. Chikazumi, J. Phys. Soc. Jpn. 39, 839 (1975).

[12]O. Steinsvoll, L. M. Corliss, and J. M. Hastings (unpublished).

[13]E. J. Samuelsen and O. Steinsvoll, Phys. Status Solidi B 61, 615 (1974).

[14]M. J. Cooper and R. Nathans, Acta Crystallogr. 23, 357 (1967).

[15]R. Comès, M. Lambert, and A. Gunier, Solid State Commun. 6, 715 (1968).

[16]The phase of the displacements of equivalent atoms on different layers is governed by $\sin[\pi(z_i - z_j)]$, where i and j correspond to the different layers along the z direction.

[17]J. Skalyo, Jr., G. Shirane, S. A. Friedberg, and H. Kobayashi, Phys. Rev. B 2, 1310 (1970).

[18]Y. Yamada, H. Takatera, and D. L. Huber, J. Phys. Soc. Jpn. 36, 641 (1974).

[19]K. N. Pak and W. Kinase, J. Phys. Soc. Jpn. 38, 1 (1975).

[20]K. Kobayashi, J. Phys. Soc. Jpn. 24, 497 (1968).

[21]Y. Yamada, Y. Noda, J. D. Axe, and G. Shirane, Phys. Rev. B 9, 4429 (1974).

[22]E. Pytte, Phys. Rev. B 8, 3954 (1973).

[23]W. Kündig and R. S. Hargrove, Solid State Commun. 7, 223 (1969).

[24]S. Chikazumi, in Proceedings of the Twenty-First Annual Conference on Magnetism and Magnetic Materials, Philadelphia, 1975 (unpublished).